A Stable Schrödinger-Poisson Solver to Investigate Quantum Effects in Modern MOSFETs

C. Troger, H. Kosina, and S. Selberherr

Institute for Microelectronics, TU Vienna, Gusshausstrasse 27–29, A-1040 Vienna, Austria
Phone +43/1/58801-36013, FAX +43/1/58801-36099, e-mail troger@iue.tuwien.ac.at

1 Introduction

As a consequence of continuous scaling of MOS devices and the resulting high transverse electric fields at the interface, a reliable device simulation tool has to account for the quantized states in the channel. From a methodological point of view it seems favorable for the simulation of complete devices to consider the quantization effects by one-dimensional cuts perpendicular to the interface [1], or to introduce a quantum mechanical correction in classical device simulation. In this view we compare the results from an advanced solver for Schrödinger's equation to a commonly used correction for the classical electron density.

2 Formulation

2.1 Schroedinger Equation

For the description of the quantum mechanical charge in a two-dimensional electron gas it is common practice to separate the wave function $\Psi(\mathbf{r})$ into a plane wave parallel to the interface and an envelope function $\psi(z)$. Following the effective mass approach and including the nonparabolicity correction in the bulk dispersion relation we have to solve the one-dimensional Schrödinger equation.

$$\left(\hat{\mathbf{T}} + \hat{\mathbf{V}}\right)\psi(z) = E\,\psi(z) \qquad (1)$$

The Operator $\hat{\mathbf{V}}$ is defined by the confining potential, $\hat{\mathbf{T}}$ is the operator of the kinetic energy and K is the wave vector of the plane wave parallel to the interface.

$$\hat{\mathbf{T}} + \hat{\mathbf{T}}\alpha\hat{\mathbf{T}} = \frac{\hbar^2}{2}\left(\frac{K^2}{m_{||}} - \frac{\partial}{\partial z}\frac{1}{m_z}\frac{\partial}{\partial z}\right) \qquad (2)$$

An analytical treatment of the operator $\hat{\mathbf{T}}$ has to be performed in the eigenfunction space of the operator

$$\hat{\mathbf{G}} = \frac{K^2}{m_{||}} - \frac{\partial}{\partial z}\frac{1}{m_z}\frac{\partial}{\partial z}. \qquad (3)$$

If the material parameters m_z and $m_{||}$ are assumed to be independent of position and we neglect the penetration of the wave function in the oxide, a good basis for this calculations can be found in form of a sinus series expansion of the wave functions. Nevertheless the method described in this paper is not restricted to this assumptions and can even be expanded to heterostructures.

As a consequence the spectral representation $\mathbf{a}$ of the envelope function $\psi(z)$ for a specific value of the magnitude K of the in-plane wave vector is then obtained as the solution of the matrix eigenvalue problem $(\mathbf{T} + \mathbf{V})\,\mathbf{a} = E_n\,\mathbf{a}$, where T and V stand for matrices comprising the matrix elements of the operator for the kinetic and potential energy.

2.2 In-plane Dispersion Relation

For any calculation involving the density of states an analytic in-plane dispersion relation is very useful. Similar to the method used in [2] perturbation theory is used to derive an explicit expression for the wave function and the eigenenergies for each subband in terms of K. The operator of the kinetic energy is expanded in a Taylor series in K^2, and only the terms

$$\begin{aligned} T_0 &, \\ T_1 &= \frac{1}{m_{||}} T'\left(\frac{-1}{m_z}\frac{\partial^2}{\partial z^2}\right), \\ T_2 &= \frac{1}{2m_{||}^2} T''\left(\frac{-1}{m_z}\frac{\partial^2}{\partial z^2}\right) \end{aligned} \tag{4}$$

are retained to obtain a parameter set consisting of eigenenergy E_n, nonparabolicity α_n and mass m_n for each subband. Hence, we define the in-plane dispersion relation $\mathcal{E}_n$ for the n-th subband implicitly as

$$(\mathcal{E}_n - E_n)\left(1 + \alpha_n(\mathcal{E}_n - E_n)\right) = \frac{\hbar^2 K^2}{2m_n}. \tag{5}$$

$$\begin{aligned} m_n &= \frac{\hbar^2}{2T_{1,nn}} \\ \alpha_n &= -\frac{1}{T_{1,nn}^2}\left(T_{2,nn} + \sum_{m\neq n}\frac{|T_{1,mn}|^2}{E_n^0 - E_m^0}\right) \end{aligned} \tag{6}$$

Beside the perturbation theory of second order, the above coefficients are calculated without further approximations and the given in-plane dispersion relation can be considered as a consistent inclusion of nonparabolicity for the transport simulation of a quasi two-dimensional electron gas.

2.3 Self Consistent Iteration

The potential is calculated by means of a finite difference discretization of Poisson's equation

$$\frac{d}{dz}\epsilon\frac{d}{dz}\phi(z) = e\left(p(z) - n(z) + C(z)\right). \tag{7}$$

To solve equation (7) a Newton iteration is used and we therefore need an estimation for the derivative of the electron concentration with respect to the potential. In general the electron concentration can be expressed as

$$\begin{aligned} n(z) &= \sum_n |\psi_n(z,K)|^2 f(E_n) \\ f(E_n) &= \frac{m_n k_B T}{\pi\hbar^2}\log\left(\frac{1+\exp\left[\frac{E_f - E_n}{k_B T}\right]}{1+\exp\left[\frac{E_f - E_{lim}}{k_B T}\right]}\right) \end{aligned} \tag{8}$$

Following the method given in [3] the derivative of the electron concentration with respect to the potential energy can be found. After some calculation, where the deviation of δn resulting from a potential change δV is calculated by perturbation theory, we finally get

$$\delta n = -e\sum_n |\psi_n(z,K)|^2 \frac{\partial f}{\partial E_n}\delta V \tag{9}$$

This result gives a surprisingly simple formula for the derivative of the squared wave function with respect to the potential energy and removes the nonlocal effect introduced by Schrödinger's equation.

For the calculation of the electron concentration the energy domain is split into two parts at E_{lim} which is chosen after the calculation of the eigenenergy levels. Only electrons with energies below this energy were treated in a quantum mechanical fashion. This procedure is useful to simulate electron accumulation that forms in the source and drain region of a MOS device. Figure 1 shows the contributions of both parts to the total electron concentration.

3 Results

For the calculation of realistic CV characteristics of MOSFETs the model was extended to cover a polygate in the simulation. Figure 2 and 3 show the resulting CV-Curves obtained for different calculations of the electron concentration with and without polygate. In each case we used the classical equilibrium concentration for Fermi Dirac

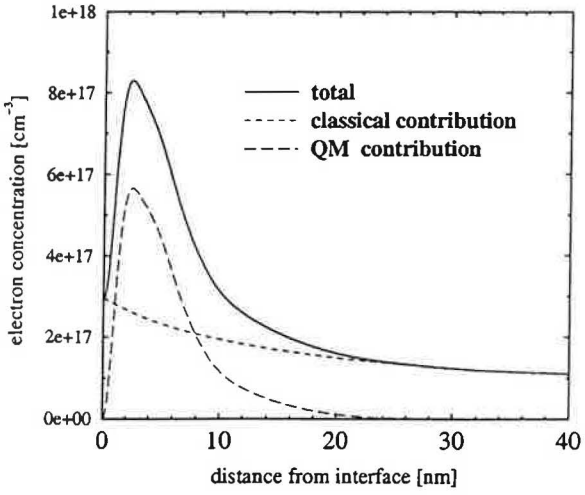

Figure 1: Classical and quantum mechanical (QM) contribution to the electron concentration in an accumulation layer

statistics (classical), a commonly used correction as proposed by Hänsch in [4] (corrected) and the quantum mechanical method (QM). The doping of the polygate is $5 \cdot 10^{19}$ cm^{-3}, the chosen $t_{ox} = 2.5$ nm and the channel doping $5 \cdot 10^{17}$ cm^{-3}. For both cases the corrected classical model results in a threshold voltage shift of approximately 50 mV compared to 70 mV in the quantum mechanical case. In Figure 4 and 5 we plot the relative error for the electron concentration that is found between the corrected classical formula and the quantum mechanical calculation. The error is plotted for different applied gate-bulk voltages and an oxide thickness of 2.5 nm. The doping of the retrograde well for the metal gate (Figure 4) changes from $10^{17} cm^{-3}$ to $4 \cdot 10^{17}$ cm^{-3} at a depth of 15 nm, whereas for the polygate (Figure 5) the two doping concentrations were chosen as $2 \cdot 10^{17}$ cm^{-3} and $6 \cdot 10^{17}$ cm^{-3}. For different doping levels and profiles we always find a situation similar to the given figures. The electron concentration is overestimated by up to 30 % to 70 % in the range of the first subband. For larger values of z the classical correction seems to miss the contribution of the higher subbands. In this region the error can reach some -300 %, which is quite larger than the typical error of less than 80 % found for larger oxide thickness and lower channel doping. Nevertheless in this region the electron concentration decreases rapidly and the effect on relevant physical quantities is thus quite small.

4 Conclusion

The presented Schrödinger Poisson solver can be used to calculate both accumulation and inversion in a MOSFET device. Both stability and con-

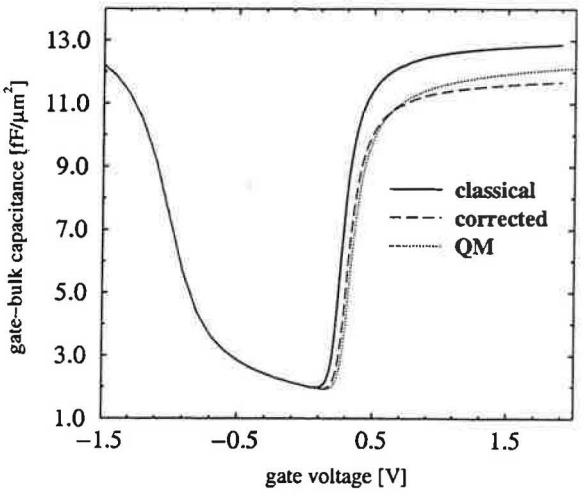

Figure 2: CV-curves for metal gate

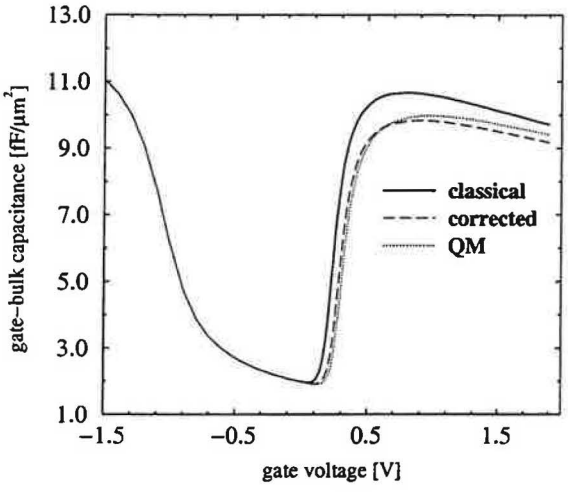

Figure 3: CV-curves for polygate

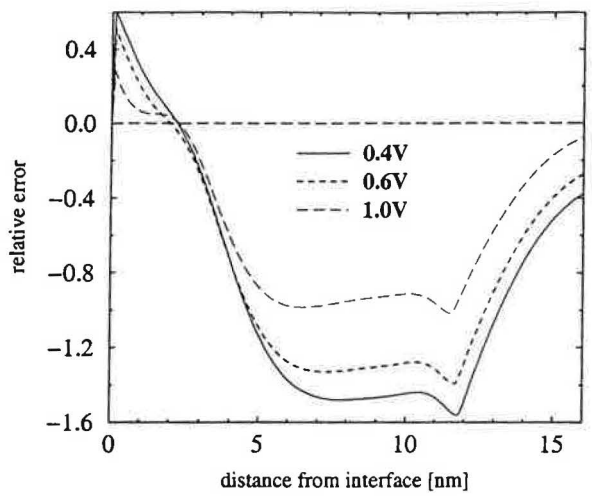

Figure 4: Difference in electron concentration for metal gate and retrograde well

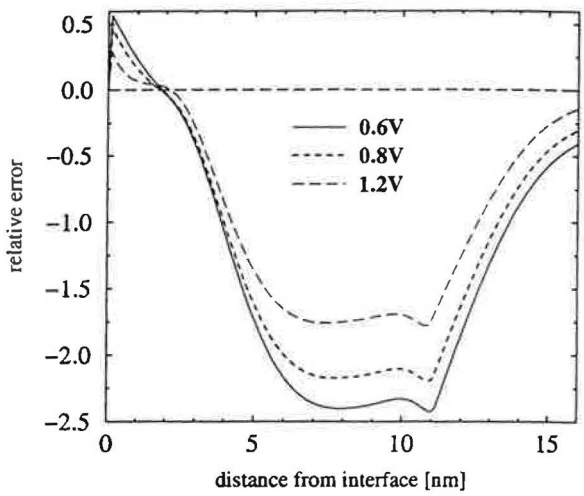

Figure 5: Difference in electron concentration for polygate and retrograde well

vergence speed have been improved by calculating the derivative of the electron concentration with respect to the potential from the wave functions.

The Hänsch correction of the classical electron concentration has been compared to the self consistent quantum mechanical calculation and was found to be also useful for the next generation of MOSFET devices.

ACKNOWLEDGMENT

This work has been partly supported by the "Österreichischer Akademischer Austauschdienst" project : *STONES - 11/98*. Fruitful discussion with F. Gamiz are acknowledged.

References

[1] A. Spinnelli, A. Benvenuti, and A. Pacelli, "Self Consistent 2-D Model for Quantum Effects in n-MOS Transistors," *IEEE Trans.Electron Devices*, vol. ED-45, no. 6, pp. 21342–1349, 1998.

[2] M.V. Fischetti and S.E. Laux, "Monte Carlo Study of Electron Transport in Silicon Inversion Layers," *Physical Review B*, vol. 48, no. 4, pp. 2244–2274, 1993.

[3] A. Trellakis, A.T. Galick, A. Pacelli, and U. Ravaioli, "Iteration Scheme for the Solution of the two-dimensional Schroedinger-Poisson Equation in Quantum Structures," *J.Appl.Phys.*, vol. 81, no. 12, pp. 7880–7884, 1997.

[4] W. Hänsch, Th. Vogelsang, R. Kircher, and M. Orlowski, "Carrier Transport near the Si/SiO_2 Interface of a MOSFET," *Solid-State Electron.*, vol. 32, no. 10, pp. 839–849, 1989.